Supplementary Information for

Harnessing lanthanides for blue-to-UVB upconversion and its dye-sensitization

Dechao Yu[1,2], Benchun Li[1], Arend Zhang[2], Jasper Pol[3], Dawei Zhang[1], Songlin Zhuang[1], and Difei Zhou*[,3,4]

[1] *Engineering Research Center of Optical Instrument and System, The Ministry of Education, Shanghai Key Laboratory of Modern Optical Systems, University of Shanghai for Science and Technology, Shanghai 200093, China*

[2] *Condensed Matter and Interfaces, Debye Institute for Nanomaterials Science, Utrecht University, Princetonplein 5, 3584 CC Utrecht, The Netherlands*

[3] *Stratingh Institute for Chemistry, University of Groningen, Nijenborgh 4, 9747 AG Groningen, The Netherlands*

[4] *Symeres Netherlands B.V., Kadijk 3, 9747 AT Groningen, The Netherlands*

*Address correspondence to Difei Zhou, email: difei.zhou@symeres.com

Experimental

1. Chemicals:

All chemicals were used without further purification. YF_3 (99.99%), HoF_3 (99.9%), and GdF_3 (99.99%) were purchased from ChemPUR company. NaF (≥ 98%), NH_4F (≥ 98%), NaOH (> 97%), Yttrium acetate hydrate (99.9%, $Y(Ac)_3.xH_2O$), Gadolinium acetate hydrate (99.9%, $Gd(Ac)_3.xH_2O$), Holmium acetate hydrate (99.99%, $Gd(Ac)_3.xH_2O$), Cyclohexane (99.5%, CH), Oleic acid (90%, OA), 1-octadecene (90%, ODE), Ethanol (> 99.8%, EtOH), Methanol (> 99.85%, MeOH), Tetrahydrofuran (≥99.9%, anhydrous, inhibitor-free; THF) were all purchased from Sigma-Aldrich company.

2. Synthesies of $NaYF_4$:*x*%Ho^{3+},*y*%Gd^{3+} (*x*=1, 3, 7; *y*=10, 25, 93), and $NaYF_4$:*x*%Ho^{3+},25%Gd^{3+} (*x*=0.1, 0.3, 0.5, 0.7, 5) bulk particles by solid-state reaction

The synthesis method of Aarts *et al.*[1] was here introduced as a starting point: the starting materials of NaF (5% excess) and YF_3 were mixed with NH_4F, which then were ground completely and then transferred to an alumina crucible; following an additional crucible with NH_4F was placed at the entrance of a tube oven to create a fluoride-rich atmosphere, the above mixture was sintered under nitrogen atmosphere, first at 300 °C for 2 hours and then at 550 °C for 3 hours.

When using this synthesis method for $NaYF_4$:Ho^{3+},Gd^{3+} phosphors (i.e., GdF_3 and HoF_3 precursors used to replace part of YF_3 precursor), we employed a 20% excess of NaF in the starting materials, and increased the reaction temperature to 600 °C for a longer holding time of 10 hours. Practically this will make a well crystallized phase pure products with a successful substituation of Gd^{3+} dopant in the Y^{3+} sub-lattice sites (radium of Gd^{3+} ~ 1.247 Å lager than that of Y^{3+} ~ 1.215 Å in the 9-fold coordination of β-$NaYF_4$ host),[2,3] especially for a high Gd^{3+} dopant concentration like more than 25% (otherwise significant amounts of unreacted GdF_3 precursor remain). On the other hand, it was also found that it is important to dry the precursors before weighing them, as the hygroscopic nature of some precursors may otherwise result in non-stoichiometric reaction mixtures.

3. Synthesies of $NaYF_4$ and $NaYF_4$:*x*%Ho^{3+},25%Gd^{3+} (*x*=1, 3, 5, 8, 10, 12, 15) NPs by thermolysis procedures

Nanoparticles (NPs) of $NaYF_4$ and $NaYF_4$:*x*%Ho^{3+},25%Gd^{3+} were synthesized using a typical thermolysis procedure modified according to the protocol announced by Wang *et al.*[4] and that by Ma *et al.*[5] To syntheize 1 mmol $NaYF_4$ product, 1 mmol $Y(Ac)_3.xH_2O$ were weighed and mixed with 4 mL OA and 11 mL ODE in a 50 mL round bottom three-neck flask using a Teflon-coated oval magnetic stir bar. Following the connection of the flask with condeser to a Schlenk line with a dual vacuum/N_2 gas manifold, the mixed solution was gradually heated up to 135 °C under vacuum and vigorous stirring, and kept for 30 minutes until it became clear. With gentle flow of N_2 gas, through the reaction flask, the solution cooled down to temperature below 40 °C, and then 10 mL MeOH solution dissolved with

2.5 mmol NaOH and 4 mmol NaF was injected into the flask with vigorous stirring for more than 30 miunutes. Subsequently, the resulting white turbid reaction mixture was slowly heated up to 100 °C under vaccum to evaporate methonal for about 10 minutes, and continously to 135 °C to remove all the residula water for 20 minutes. After 3 times flushes between vacuum and N_2 gas, the solution was finally heated to 300 °C in N_2 atomsphere, and kept for 2 hours for complete raction and crystal growth. After reaction and cooling down to room temperature, the slightly turbid reaction mixture was transferred to a 40 mL glass vial, and washed to remove excess reagents and solvents. This was done by adding 1 equivalent of EtOH, centrifuging with a revolutions per minute (RPM) of 3000 for 10 minutes and removing the supernatant. The resulting sediment was redispersed in 5 mL CH. This washing step was repeated two more times to obtain a clear and colorless dispersion of nanocrystals in 5 mL CH. To synthesize $NaYF_4$:*x*%Ho^{3+},25%Gd^{3+} NPs, the nominal ratio of $Ho(Ac)_3.xH_2O$ and that of $Gd(Ac)_3.xH_2O$ replace the parts of $Y(Ac)_3.xH_2O$ as dopants in the final products $NaY_{0.75-x\%}Ho_{x\%}Gd_{0.25}F_4$, and all the other precedures are same to the above synthesis.

4. Synthesis of 3-ethoxy-3-oxo-2-(perylen-3-ylmethyl)propanoic acid (PPA2)

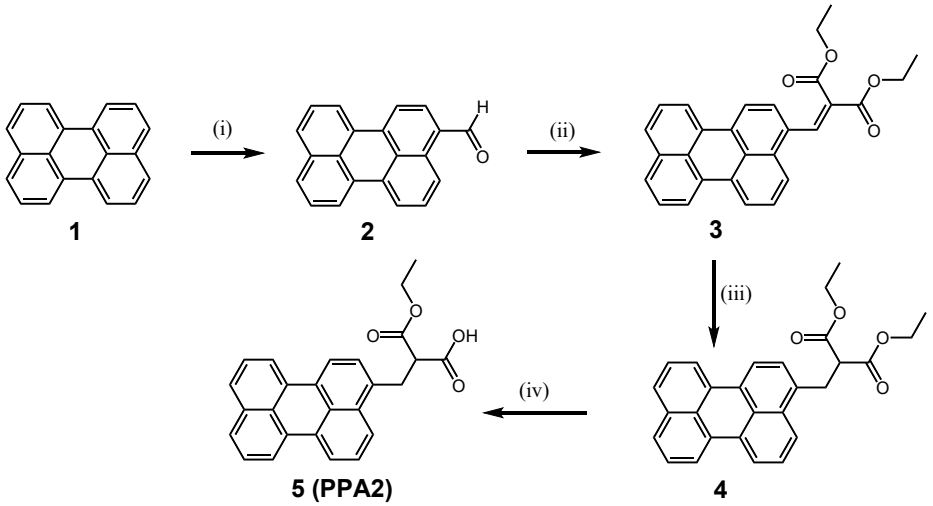

Scheme 1. (i) Titanium tetrachloride, 1,1-dichloromethyl methyl ether, *o*-dichlorobenzene. (ii) Diethyl malonate, piperidine, toluene. (iii) Zinc, acetic acid. (iv) Sodium hydroxide, water, tetrahydrofuran, hydrochloride.

Perylene-3-carbaldehyde (**2**). Compound **2** was synthesized from perylene with a procedure modified from literature.[6] A N_2-filled, dry flask was filled with perylene (3.0 g, 12 mmol) and then placed in an ice-water bath. Anhydrous o-dichlorobenzene (50 mL) was then added, followed by the addition of 1,1-dichloromethyl methyl ether (1.63 mL, 18 mmol). Finally titanium tetrachloride was added dropwise. After 1 hour, the ice bath was removed. The reaction proceeded at room temperature for 1 hour, then the resulting mixture was poured into 200 mL of demineralized water with 2 mL concentrated HCl. Chloroform was used to extract the product from the aqueous suspension. The organic phase was then concentrated under vacuum, and purified with silica gel column chromatography, with an eluent of

$CHCl_3$:dichloromethane (volume ratio, 1:7). The product was finally recrystallized from hot $CHCl_3$, and formed red crystals was collected and dried (2.3 g, 70% yield). 1H NMR (400 MHz, $CDCl_3$) δ 10.29 (s, 1 H), 9.13 (d, 1 H, J = 8 Hz), 8.27-8.22 (m, 4 H), 7.89 (d, 1 H, J = 8 Hz), 7.79 (d, 1 H, J = 8 Hz), 7.73 (d, 1 H, J = 8 Hz), 7.66 (t, 1 H, J = 8 Hz), 7.54-7.50 (m, 2 H).

Diethyl 2-(perylen-3-ylmethylene)malonate (**3**). Compound **3** was synthesized following a procedure modified from literature.[7] A N_2-filled dry flask was filled with Compound 2 (950 mg, 3.4 mmol), followed by the addition of toluene (15 mL), diethyl malonate (0.72 mL, 4.5 mmol), and piperidine (0.33 mL, 3.4 mmol). The reaction mixture was then refluxed for 24 hours. Afterwards the mixture was cooled down to room temperature, and water was extracted using dichloromethane. The organic phase was condensed under vacuum, and purified with silica gel column chromatography with an eluent of toluene:dichloromethane (volume ratio, 1:1). The product was collected as a red solid (1.1 g, 78% yield). 1H NMR (400 MHz, CDCl3) δ 8.40 (s, 1 H), 8.28-8.21 (m, 3 H), 8.14 (d, 1 H, J = 8 Hz), 7.86 (d, 1 H, J = 12 Hz), 7.73 (t, 2 H, J = 8 Hz), 7.61-7.56 (m, 2 H), 7.53-7.49 (td, 2 H, J = 4 Hz, 8 Hz), 4.38 (q, 2 H, J = 8 Hz), 4.22 (q, 2 H, J = 8 Hz), 1.39 (t, 3 H, J = 8 Hz), 1.14 (t, 3 H, J = 8 Hz).

Diethyl 2-(perylen-3-ylmethyl)malonate (**4**). Compound 4 (diethyl 2-(perylen-3-ylmethyl)malonate) was synthesized according to a reported synthesis procedure.[7] A N_2-filled flask was filled with Compound 3 (1.1 g, 2.6 mmol), followed by the addition of glacial acetic acid (20 mL). Finally zinc powder (3 g, 46 mmol) was added. The reaction was refluxed for 2 hours, then it was cooled down to room temperature, and extracted using dichloromethane. The organic phase was condensed under vacuum, and purified on silica gel column chromatography with an eluent of dichlormethane. The product was collected as a yellow solid (0.98 g, 90% yield). 1H NMR (400 MHz, $CDCl_3$) δ 8.20-8.12 (m, 3 H), 8.06 (d, 1 H, J = 8 Hz), 7.85 (d, 1 H, J = 8 Hz), 7.67-7.64 (m, 2 H), 7.53 (t, 1 H, J = 8 Hz), 7.48-7.43 (td, 2 H, J = 4 Hz, 8 Hz), 7.37 (d, 1 H, J = 8 Hz), 4.18 (m, 4 H), 3.85 (t, 1 H, J = 8 Hz), 3.64 (d, 1 H, J = 8 Hz), 1.21 (t, 6 H, J = 8 Hz).

3-Ethoxy-3-oxo-2-(perylen-3-ylmethyl)propanoic acid (**5**, **PPA2**). A N_2-filled flask was filled with a tetrahydrofuran solution (50 mL) of Compound 4 (0.98 g, 2.3 mmol), and cooled down to 0 °C using an ice bath. An aqueous NaOH solution (92 mg in 8 mL demineralized water) was added dropwise within 3 minutes. The reaction proceeded for 6 hours, during which time the ice bath slowly warmed up to room temperature. The reaction mixture was then acidified with 20 mL of 1 N HCl in water. The resulting suspension was then extracted with ethyl acetate. The organic phase was collected and condensed under vacuum. The obtained solid was purified on silica gel column chromatography, with an eluent of dichloromethane/tetrahydrofuran/acetic acid (volume ratio, 1:0.05:0.005). The product was collected as a yellow solid (350 mg, 38% yield). 1H NMR (400 MHz, $CDCl_3$) δ 8.22-8.13 (m, 3 H), 8.08 (d, 1 H, J = 8 Hz), 7.85 (d, 1 H, J = 8 Hz), 7.68-7.65 (m, 2 H), 7.54 (t, 1 H, J = 8 Hz), 7.49-7.44 (td, 2 H, J = 4 Hz, 8 Hz), 7.38 (d, 1 H, J = 8 Hz), 4.18 (m, 2 H), 3.90 (t, 1 H, J = 8 Hz), 3.67 (d, 1 H, J

= 8 Hz), 1.19 (t, 3 H, J = 8 Hz). 13C NMR (101 MHz, DMSO-d6) δ 170.27, 169.31, 134.65, 134.50, 132.91, 131.54, 130.94, 130.87, 130.02, 128.69, 128.39, 128.26, 128.18, 128.07, 127.51, 127.39, 127.32, 123.98, 121.25, 121.16, 120.95, 120.75, 61.30, 52.56, 31.95, 14.33. HRMS (ESI) m/z Found: 397.14458, calculated: 397.14344 for $C_{26}H_{21}O_4$ [M + H]+.

5. Binding of PPA2 dye molecules with NPs

According to the binding procedure developed in Prof. Hummelen's group,[8] PPA2 dye dissolved in THF was directly mixed at room temperature with $NaYF_4$ and $NaYF_4$:Ho^{3+},Gd^{3+} NPs dissolved in THF, such that an overall THF volume of 5 mL was obtained. Mass ratio of dye over NPs was designed to be 1:100, 1:200 and 1:300, respectively. For easy comparison, the mass concentration of NPs in the solution was kept constant at 3 mg/mL, while that of PPA2 dye molecules was varied to obtain the desired ratio. The mixtures were stirred for 30 minutes for complete binding.

6. Estimation of linked PPA2 dyes

The surface coverage parameters of "antenna" PPA2 dyes on the NPs are estimated using the same protocol reported by Zou *et al*.[8] Representatively, the results of the sensitized $NaYF_4$:10%Ho^{3+},25%Gd^{3+} NPs are shown in Table S1.

Table S1. Surface coverage parameters for the dye-sensitized systems.

NPs	Dye:NPs mass ratio	Average number of antennas per NP	Antenna-to-antenna distance (nm)
$NaYF_4$:10%Ho^{3+},25%Gd^{3+}	1:100	578	2.1
	1:200	288	2.9
	1:300	192	3.6

7. Photophysical setups:

Powder X-ray diffraction (XRD) patterns were measured on a Philips PW1729 X-ray diffractometer using Cu K_α radiation (λ = 1.5418 Å). Transmission electron microscopy (TEM) characterization was performed using a FEI Tecnai-12 microscope operating at 120 kV. Samples for TEM imaging were prepared by drop-casting a CH solution of washed nanocrystals onto a carbon-coated 200 mesh copper TEM grid. Absorption spectra were obtained by means of a Perkin-Elmer Lambda 950 UV/Vis/NIR spectrophotometer. Steady photoluminescence (PL) measurements (i.e., excitation, emission) were recorded on an Edinburgh Instruments FLS920 spectrofluorometer equipped with a 450 W Xenon lamp, monochromators with grating blazed at 500 nm, and a Hamamatsu R928 photomultiplier tube (PMT). PL decay curves of PPA2 dye molecules were acquired by time-correlated mono-photon counting via

time-to-amplitude conversion using a Hamamatsu photosensor module H7422-40 as a detector, while an Edinburgh EPL-405 pulsed diode laser (404.2 nm, 59.0 ps pulse width, 0.02-20 MHz repetition rate). The blue-to-UVB upconversion, as well as its decay curve monitoring upconversion wavelength at 310 nm, were measured on the FLS920 spectrofluorometer with emission monochromator with a grating blazed at 300 nm, a R928 PMT, and a tunable excitaiton source of optical parametric oscillator (OPO) Opolette HE 355II (Opotek INC.; pulse width of 10 ns, repetition rate of 20 Hz and pulse energy of ca. 3 mJ). Moreover, a continuous wave (CW) ~ 450 nm dot laser (Laserlands, maximum power output ~ 2.5 W) was utilized as excitaiton source to explore the blue-to-UVB upconversion on the above FLS920 set-up.

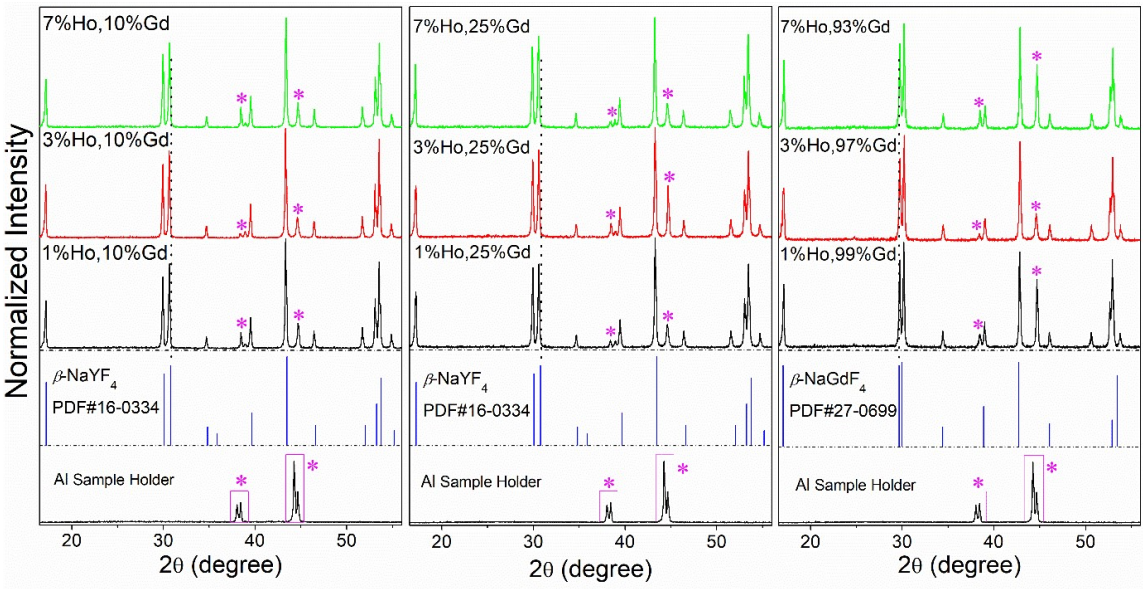

Figure S1. XRD patterns of $NaYF_4$:x%Ho^{3+},y%Gd^{3+} (x = 1, 3, 7; y = 10, 25) and $NaGd_zF_4$:Ho^{3+}_{1-z} (z = 93, 97, 99) bulk particles. The diffaction patterns of the aluminium sample holder (marked as pink stars) are also included. PDF #16-0334 and PDF #27-0699 are used as the reference patterns for the β-$NaYF_4$ and β-$NaGdF_4$ series, respectively.

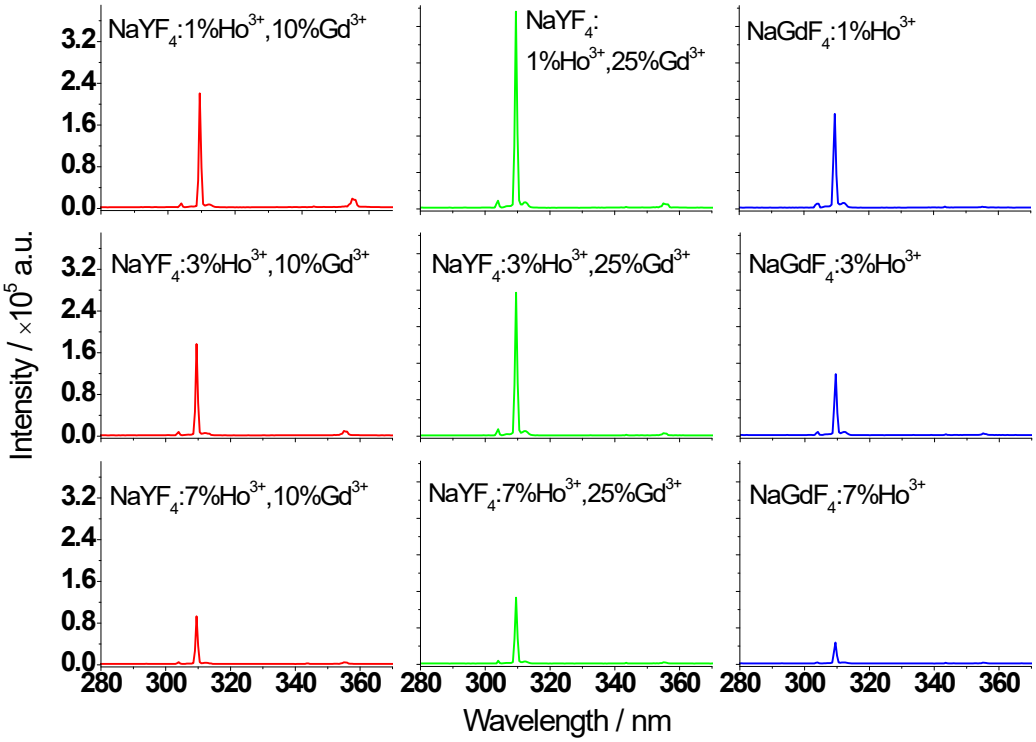

Figure S2. Blue-to-UV upconversion of a series of bulk particles pumped by an OPO laser at 447 nm.

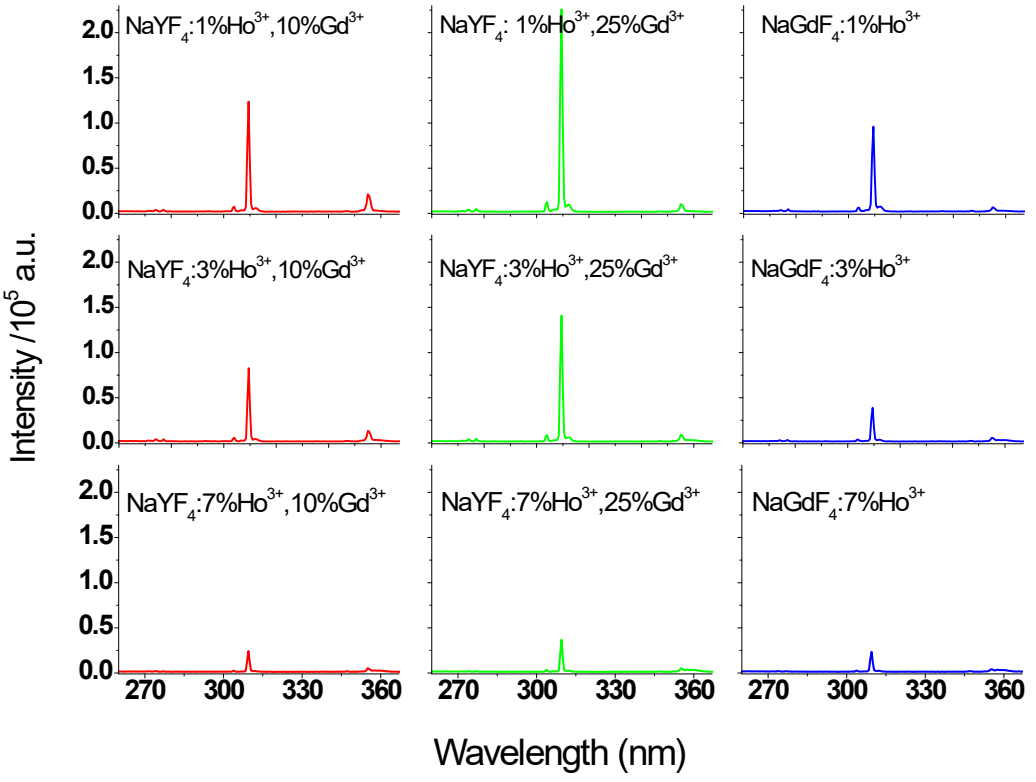

Figure S3. Blue-to-UV upconversion of a series of bulk particles pumped by a CW laser at 450 nm.

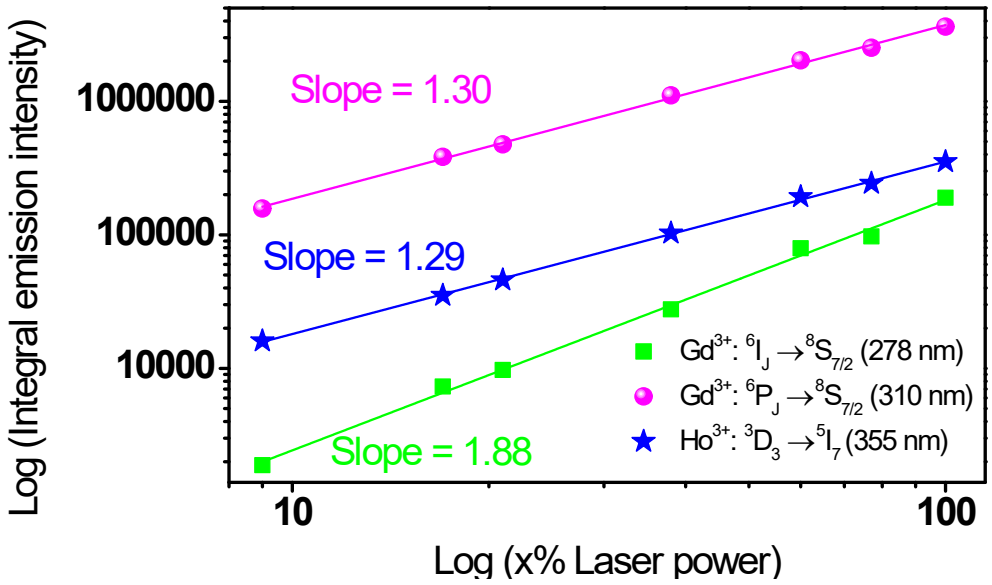

Figure S4. Logarithmic plots of the integral intensity of upconverted UV emissions as a function of laser power (excited at 447 nm) for the 278 and 310 nm of Gd^{3+} and 355 nm of Ho^{3+} in the $NaYF_4$:1%Ho^{3+},25%Gd^{3+} phosphors. Note that the observed slopes are not presenting an exact quadratic dependence. This is ascribed to the abundant energy levels and the resulting energy loss pathways in Ho^{3+}, hence the competition between upconversion and linear decay for the depletion of the intermediate excited state, which are capable of channeling the excited state energy undesirably (radiatively and non-radiatively).[9-11] In this scenario, quantum efficiencies of the emissions under discussion may be partially compromised. This would eventually translate into lower-than-2 slopes in the presented excitation power dependence. For an extensive understanding on the power dependence of upconversion, refer to the theoretical modeling reported by Ref. 9 (namely Ref. 40 in the main text).

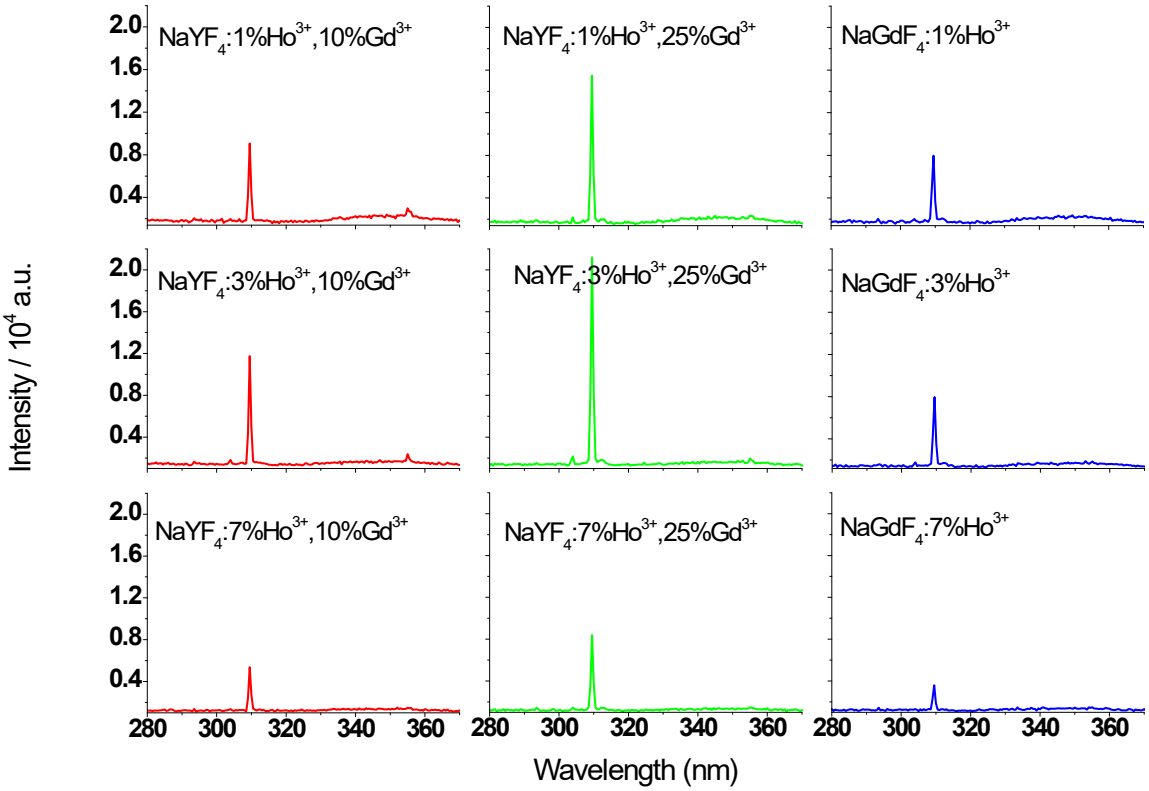

Figure S5. Green-to-UV upconversion of a seris of Ho^{3+}/Gd^{3+}-doped bulk particles pumped by an OPO laser at 535 nm.

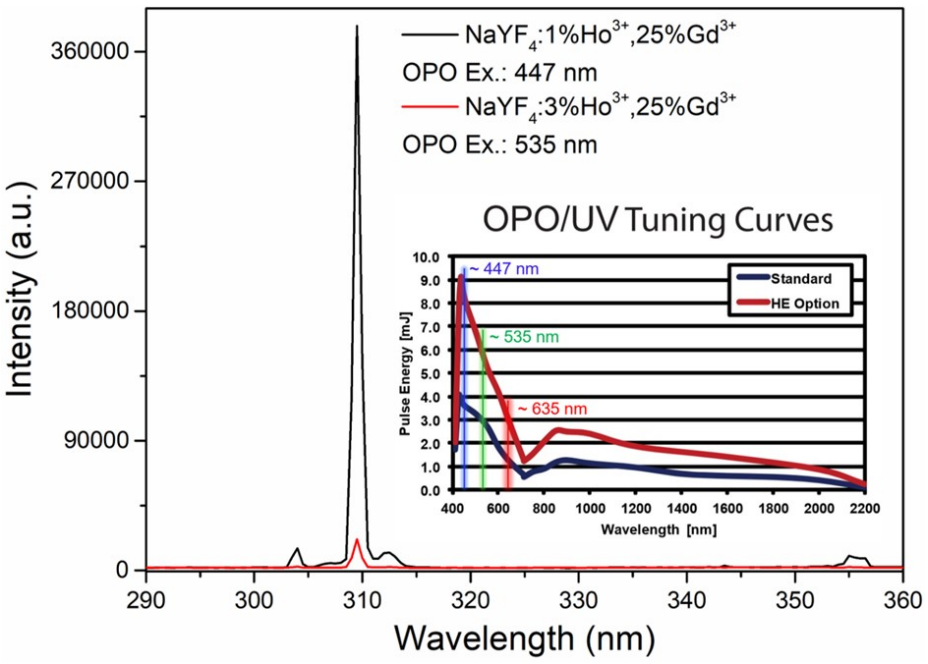

Figure S6. Comparison of the UV upconversion of bulk phosphors pumped with an OPO laser at blue ~ 447 nm and at green ~ 535 nm. The insert shows the energy output of the Opolette HE 355II as a function of wavelength (modified based on the copy of datasheet download from www.OPOTEK.com).

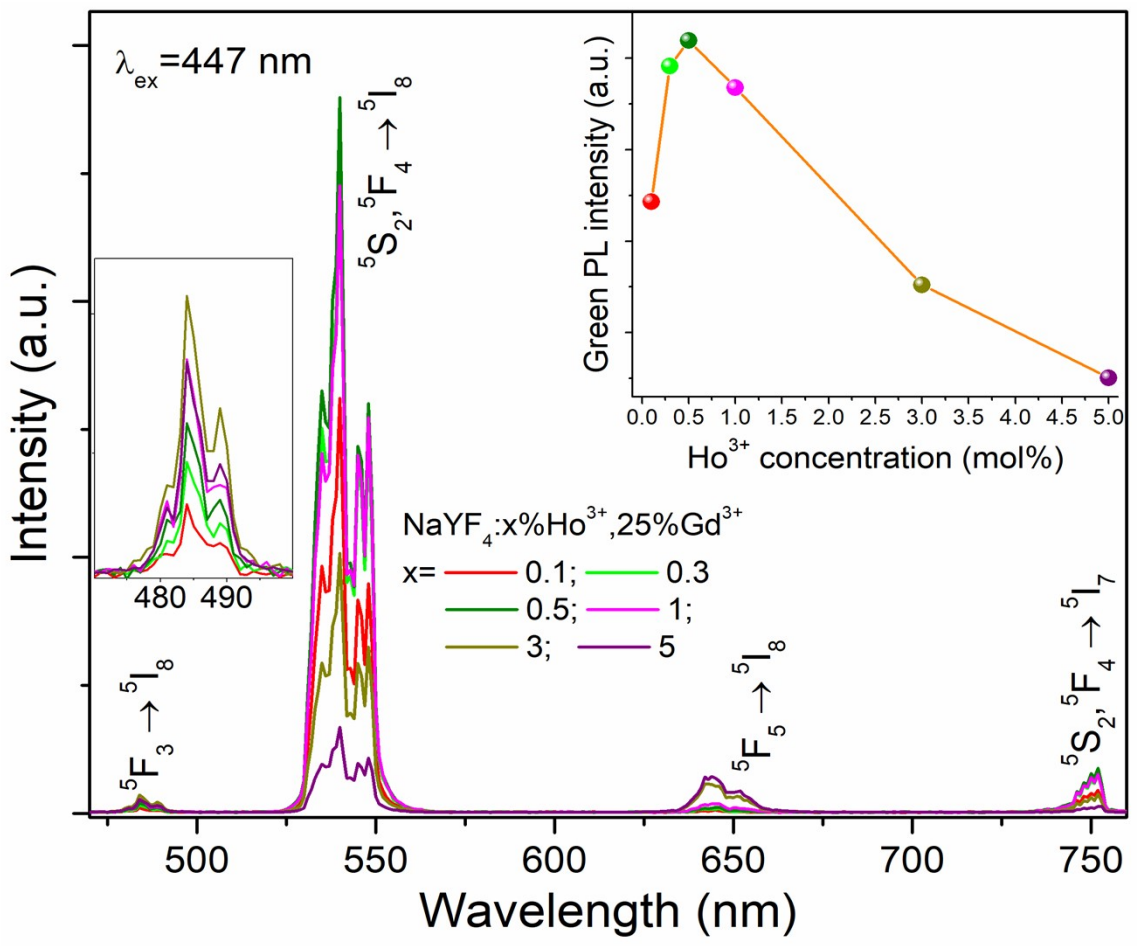

Figure S7. Photoluminescence spectra of $NaYF_4$:*x*%Ho^{3+},25%Gd^{3+} (*x*= 0.1, 0.3, 0.5, 1, 3, 5) phosphors under excitation of 447 nm. The left inset shows the magnification of Ho^{3+} concentration-dependent blue emission peak, in which it increases till 3% Ho^{3+}, and then decreases due to a competing cross-relaxation of $^5F_3 + {}^5I_8 \rightarrow {}^5F_5 + {}^5I_7$.[12] The top right inset exhibits the intensity of green emision versus Ho^{3+} concentration, where it decreases obviously once Ho^{3+} concentration moren than 0.5% because of efficient cross-relaxation of $^5S_2 + {}^5I_8 \rightarrow {}^5I_4 + {}^5I_7$ between Ho^{3+} ions.[12]

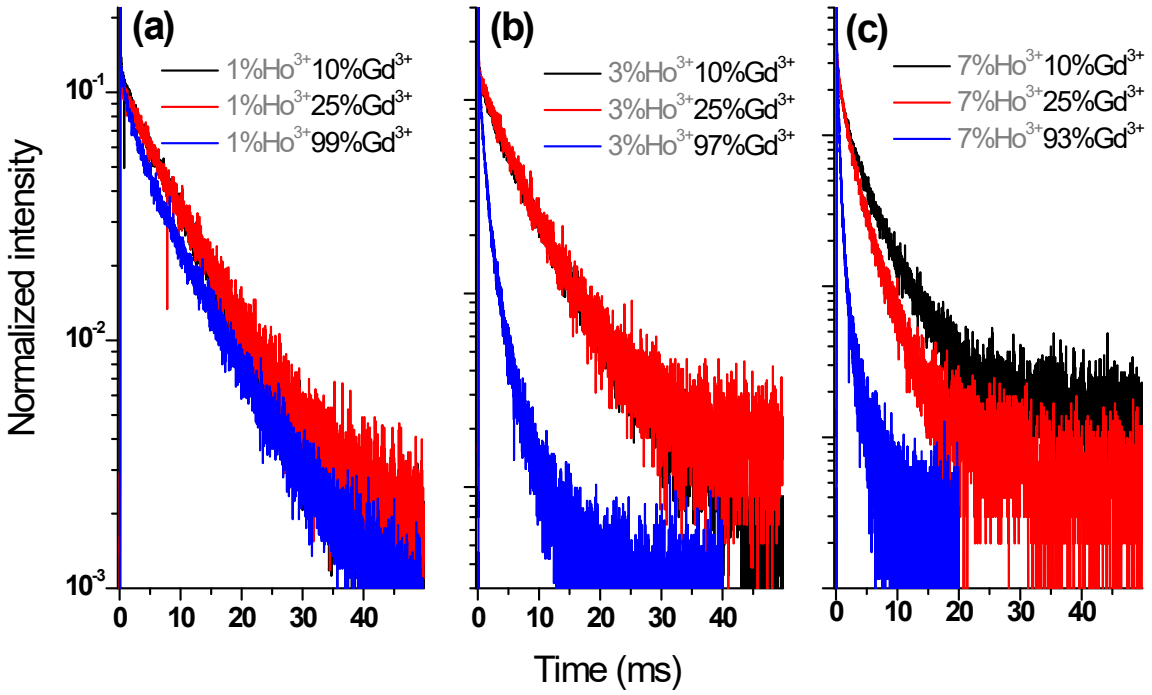

Figure S8. Decay curves of Gd^{3+}: $^6P_{7/2} \rightarrow {}^8S_{7/2}$ at 310 nm for a series of bulk particles pumped by an OPO pulsed laser at 447 nm. In the cases where the Gd^{3+}% is 10% or 25%, the phosphors have compositions of $NaYF_4$:*x*%Ho^{3+}*y*%Gd^{3+} (*x* = 1, 3, 7 and *y* = 10, 25). In the cases where the Gd^{3+}% is 93-99%, the phosphors have compositions of $NaGd_zF_4$:Ho^{3+}_{1-z}.

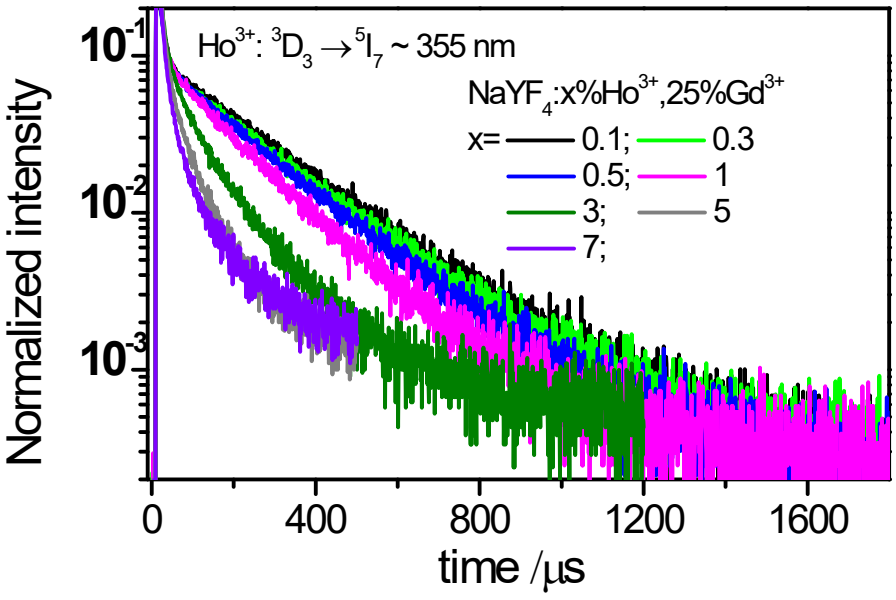

Figure S9. Decay curves of the upconverted emission at 355 nm of Ho^{3+} for $NaYF_4$:*x*%Ho^{3+},25%Gd^{3+} bulk particles.

Table S2. Exponential fittings of the decay curves of the upconverted UV emissions at 310 nm for a series of bulk particles and NPs. In case of fitting a mono-exponential decay, the fitting function is $I = A_0 \exp\left(-\frac{t}{\tau_0}\right)$, and for a bi-exponential decay, $I = A_1 \exp\left(-\frac{t}{\tau_1}\right) + A_2 \exp\left(-\frac{t}{\tau_2}\right)$. Fitting parameters are listed. For the bi-exponential decay fittings, the average decay time ($\tau_{average}$) was determined by $\tau_{average} = (A_1\tau_1^2 + A_2\tau_2^2)/(A_1\tau_1 + A_2\tau_2)$, where A_1 and A_2 are constants, τ_1 and τ_2 are the fast and slow lifetimes of the exponential components of the decay curves.

Sample	Fitting function	R^2	Component lifetime (ms)	Fitting parameter	Decay time (ms)
$NaYF_4$:0.1%Ho^{3+},25%Gd^{3+} bulk particles	Mono-	0.9678	-	A_0 ~ 0.0906	9.94
$NaYF_4$:0.3%Ho^{3+},25%Gd^{3+} bulk particles		0.9856		A_0 ~ 0.09111	9.93
$NaYF_4$:0.5%Ho^{3+},25%Gd^{3+} bulk particles		0.9905		A_0 ~ 0.08862	9.53
$NaYF_4$:1%Ho^{3+},25%Gd^{3+} bulk particles		0.9915		A_0 ~ 0.09187	8.30
$NaYF_4$:3%Ho^{3+},25%Gd^{3+} bulk particles		0.9913		A_0 ~ 0.09816	5.48
$NaYF_4$:5%Ho^{3+},25%Gd^{3+} bulk particles	Bi-	0.9977	τ_1 = 1.4644 τ_2 =4.0037	A_1 ~ 0.03445 A_2 ~ 0.06114	3.57
$NaYF_4$:7%Ho^{3+},25%Gd^{3+} bulk particles		0.9975	τ_1 = 0.8665 τ_2 =2.8681	A_1 ~ 0.05072 A_2 ~ 0.05214	2.41
$NaYF_4$:1%Ho^{3+},25%Gd^{3+} NPs	Mono-	0.9954	-	A_0 ~ 0.6682	6.85
$NaYF_4$:5%Ho^{3+},25%Gd^{3+} NPs		0.9965		A_0 ~ 0.6449	3.54
$NaYF_4$:10%Ho^{3+},25%Gd^{3+} NPs	Bi-	0.9982	τ_1 = 0.2548 τ_2 =2.3076	A_1 ~ 0.07544 A_2 ~ 0.06183	2.28
$NaYF_4$:12%Ho^{3+},25%Gd^{3+} NPs		0.9974	τ_1 = 0.3053 τ_2 =1.6006	A_1 ~ 0.1058 A_2 ~ 0.5077	1.55

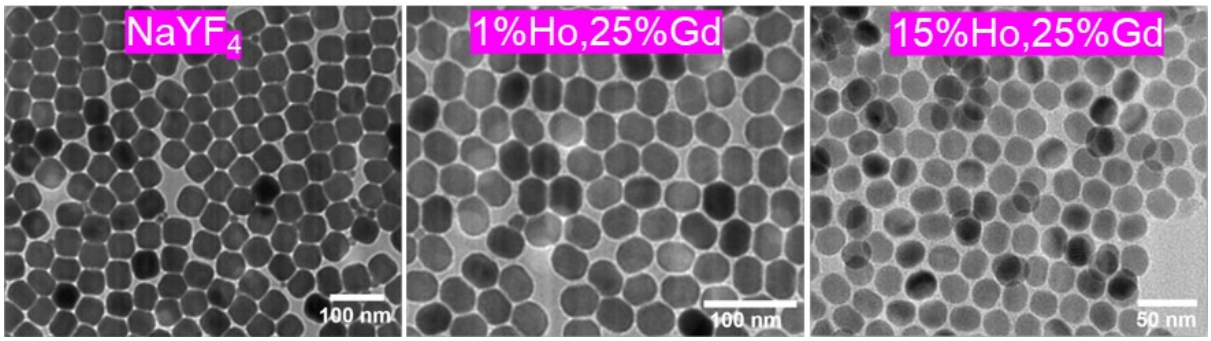

Figure S10. TEM images of $NaYF_4$ host NPs and that of $NaYF_4$:*x*%Ho^{3+},25%Gd^{3+} NPs (*x* =1, 15).

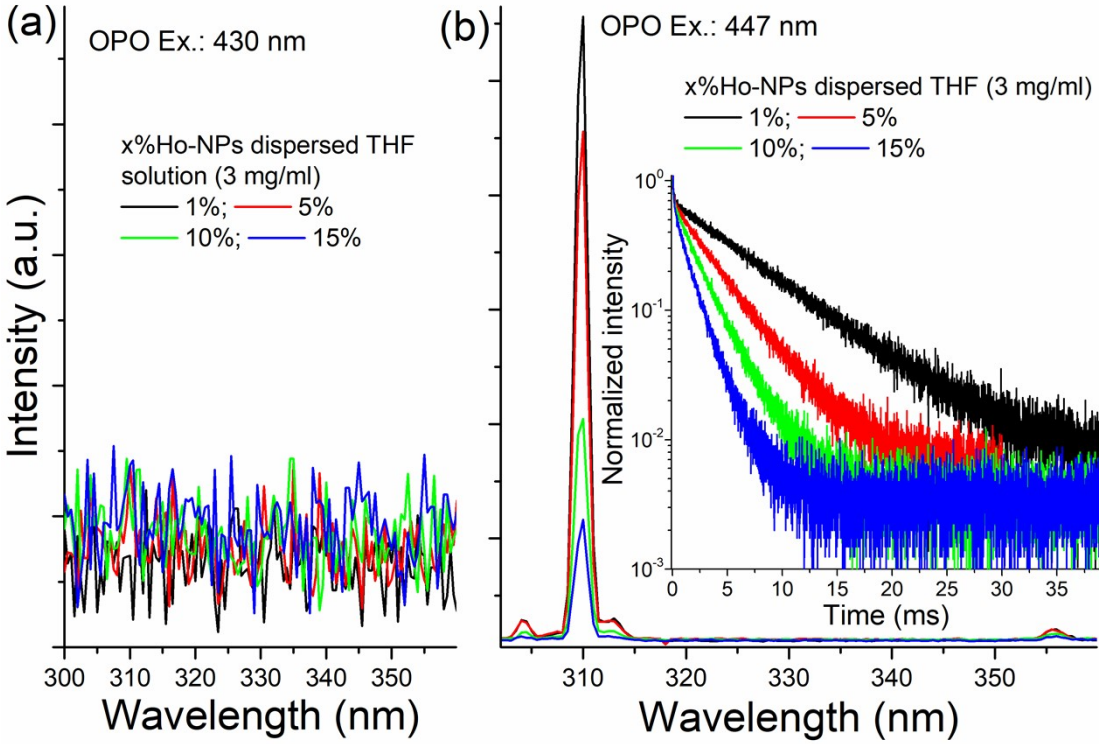

Figure S11. UV upconversion of $NaYF_4$:*x*%Ho^{3+},25%Gd^{3+} (*x* = 1, 5, 10, 15) NPs (*x*%Ho-NPs) dispersed THF solution (3 mg/ml) pumped by an OPO laser at (a) 430 nm and (b) 447 nm, respectively. Inset of Figure S12b shows the corresponding decay curves of upconverted emission at 310 nm for the *x*%Ho-NPs solutions. The faster decay trend at an elevated Ho^{3+} concentration reveals that the back energy transfer occurs from Gd^{3+} to nearby Ho^{3+} ions efficiently.

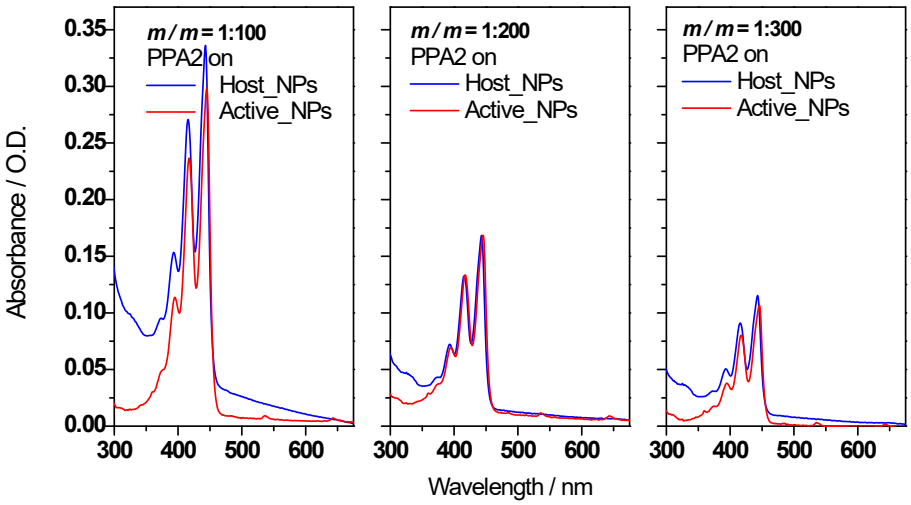

Figure S12. Absorption spectra of different PPA2-NPs solution systems. Herein Host_NPs and Active_NPs refer to $NaYF_4$ and $NaYF_4$:10%Ho^{3+},25%Gd^{3+} NPs, respectively.

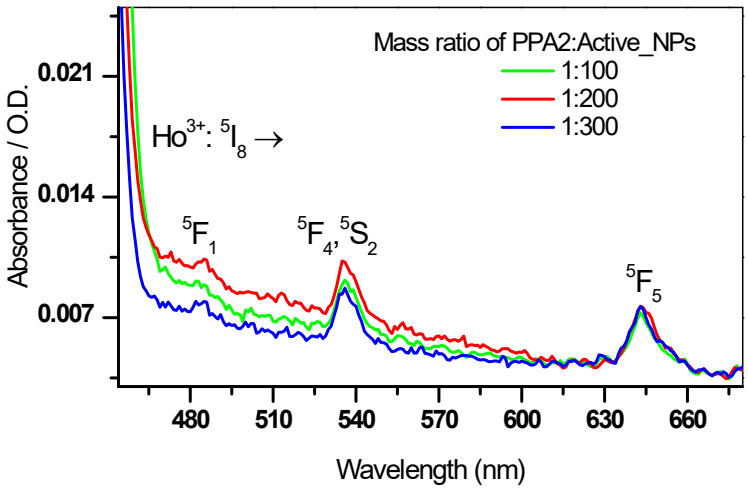

Figure S13. A zoom-in of the absorption spectra in **Figure S13**, showing the weak yet visible absorptions originating from a few of electronic transitions of Ho^{3+}, as labelled with the energy levels.

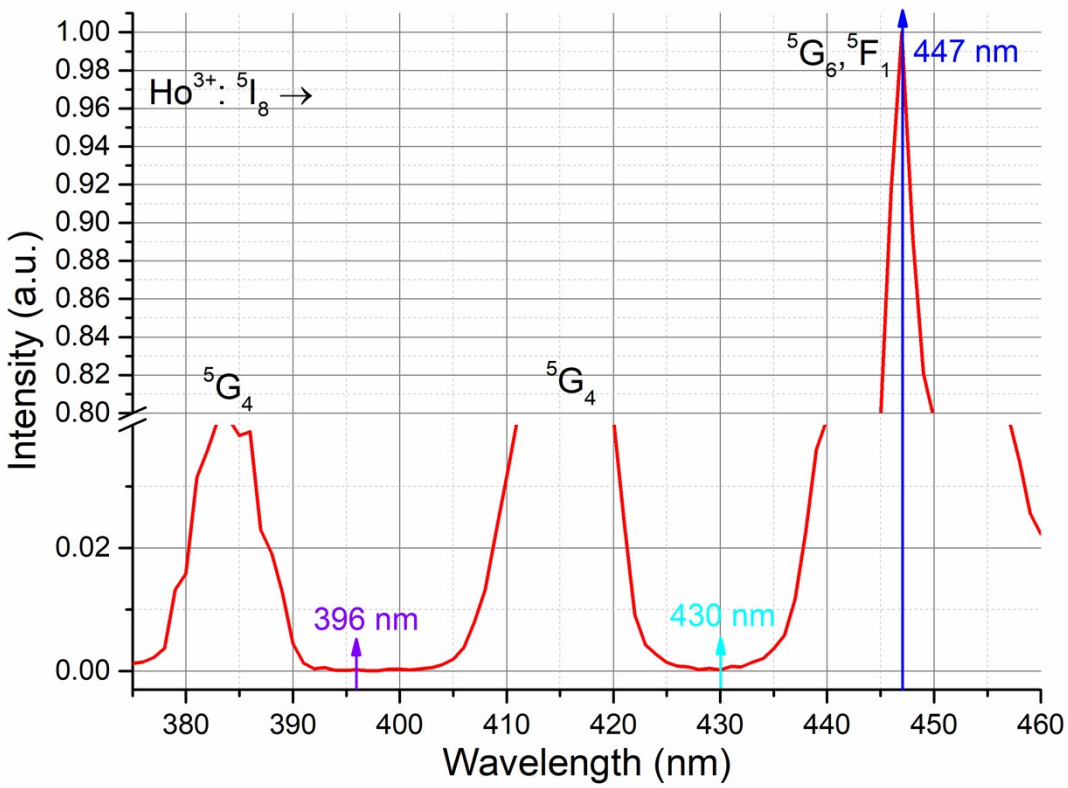

Figure S14. Magnified absorption spectrum of $NaYF_4$:1%Ho^{3+},25%Gd^{3+} bulk particles highlighting the absorption capacities at wavelengths around 396, 430 and 447 nm, respectively.

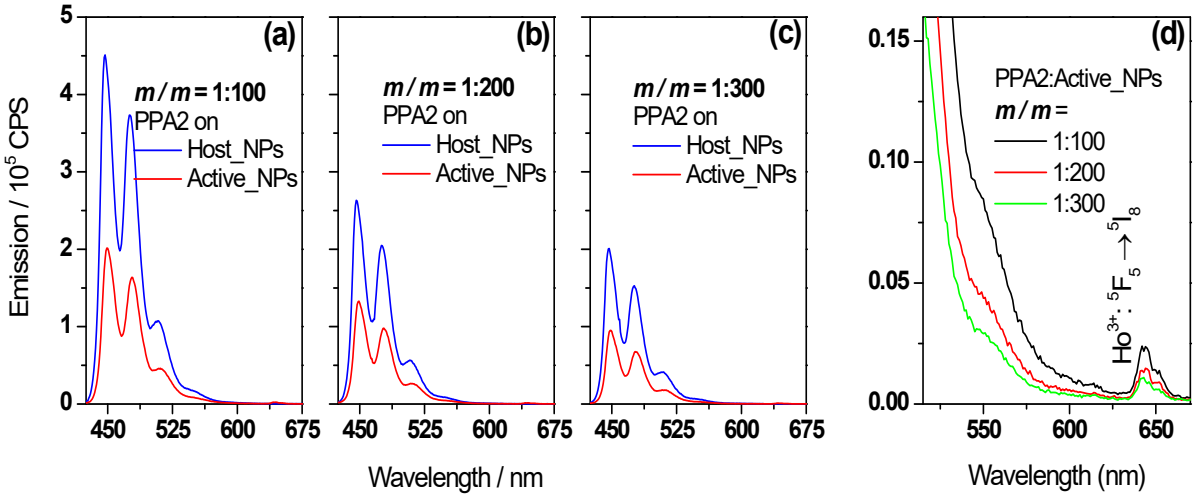

Figure S15. (a-c) Photoluminescence spectra of PPA2:NPs at different mass ratios (*m/m*) under excitaiton of 396 nm. (d) The mass ratio-related emission intensity of Ho^{3+} at about 643 nm. Host_NPs and Active_NPs refer to $NaYF_4$ and $NaYF_4$:10%Ho^{3+},25%Gd^{3+} NPs, respectively.

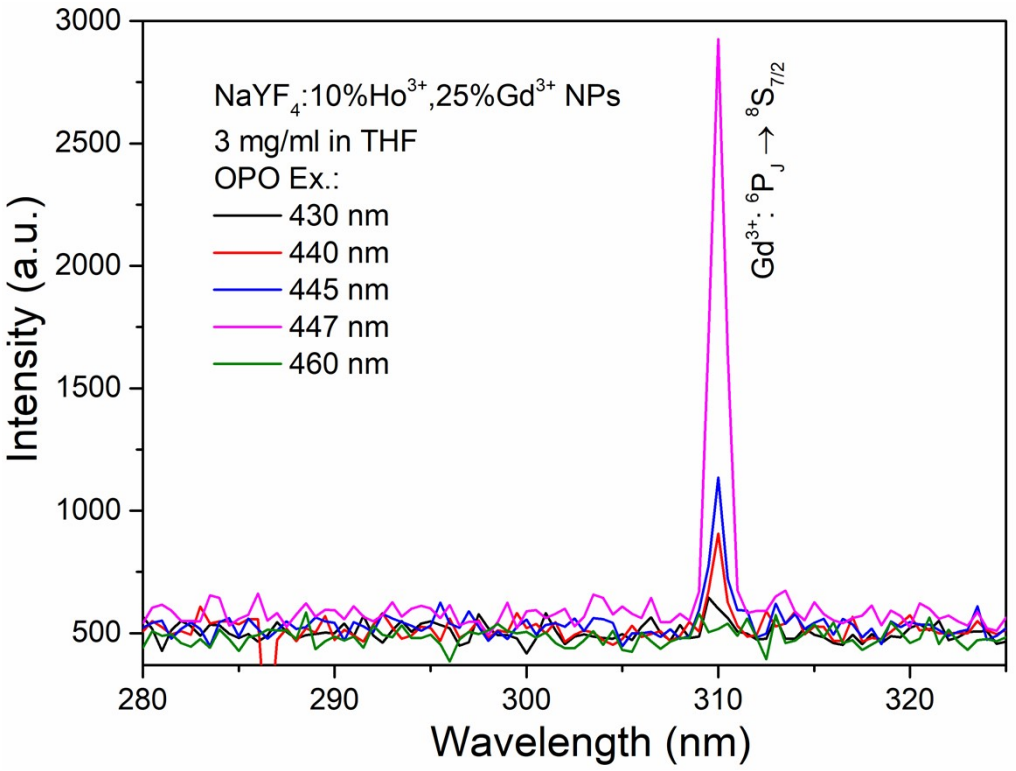

Figure S16. UVB upconversion of the $NaYF_4$:10%Ho^{3+},25%Gd^{3+} NPs dispersed in THF solution (3 mg/ml), pumped by an OPO laser at 430, 440, 445, 447 and 460 nm, respectively.

Table S3. Exponential fitting of the decay curves of PPA2 on $NaYF_4$ NPs (PPA2:Host_NPs system) and that of PPA2 on $NaYF_4$:10%Ho^{3+},25%Gd^{3+} NPs (PPA2:Active_NPs system). Fitting parameters are listed. For the bi-exponential decay fitting, the average decay time ($\tau_{average}$) was determined by $\tau_{average} = (A_1\tau_1^2 + A_2\tau_2^2)/(A_1\tau_1 + A_2\tau_2)$, where A_1 and A_2 are constants, τ_1 and τ_2 are the fast and slow lifetimes of the exponential components of the decay curves.

Mass ratio	Binding system	Fitting function	R^2	Component lifetime (ns)	Fitting parameter	Lifetime (ns)
1:100	PPA2:Host_NPs	$I = A_0 \exp(-t/\tau_0)$	0.9967	-	A_0 ~ 1.02128	4.76
	PPA2:Active_NPs	$I = A_1 \exp(-t/\tau_1) + A_2 \exp(-t/\tau_2)$	0.9974	τ_1 = 1.76126 τ_2 = 3.83013	A_1 ~ 0.71584 A_2 ~ 0.26511	2.68
1:200	PPA2:Host_NPs	$I = A_0 \exp(-t/\tau_0)$	0.9972	-	A_1 ~ 1.01274	4.53
	PPA2:Active_NPs	$I = A_1 \exp(-t/\tau_1) + A_2 \exp(-t/\tau_2)$	0.9975	τ_1 = 2.55748 τ_2 =5.8859	A_1 ~ 0.86243 A_2 ~ 0.11131	3.32
1:300	PPA2:Host_NPs	$I = A_0 \exp(-t/\tau_0)$	0.9971	-	A_0 ~ 0.98234	4.44
	PPA2:Active_NPs	$I = A_1 \exp(-t/\tau_1) + A_2 \exp(-t/\tau_2)$	0.9966	τ_1 = 2.8837 τ_2 =10.2512	A_1 ~ 0.99231 A_2 ~ 0.0334	3.64

References

1. Aarts, L.; van der Ende, B. M.; Meijerink, A. Downconverion for solar cells in $NaYF_4$:Er,Yb. *J. Appl. Phys.* **2009**, *106*, 023522.
2. Shannon, R. D. Revised effective ionic radii and systematic studies of interatomic distances in halides and chalcogenides. *Acta Cryst. A* **1976**, *32*, 751-767.
3. Vegard, L. Die konstitution der mischkristalle und die raumfüllung der atome. *Z. Phys.* **1921**, *5*, 17-26.
4. Wang, F.; Deng, R. R.; Liu, X. G. Preparation of core-shell $NaGdF_4$ nanoparticles doped with luminescent lanthanide ions to be usd as upconversion-based probes. *Nat. Protoc.* **2014**, *9*, 1634-1644 (2014).
5. Ma, C.;Xu, X.; Wang, F.; Zhou, Z.; Wen, S.; Liu, D.; Fang, J.; Lang, C. I.; Jin, D.Probing the interior crystal quality in the development of more efficient and smaller upconversion nanoparticles. *J. Phys. Chem. Lett.* **2016**, *7*, 3252-3258.
6. Ning, X.; Lee, S.; Wang, Z.; Kim, D.; Stubblefield, B.; Gilbert, E.; Murthy, N. Maltodextrin-based imaging probes detect bacteria in vivo with high sensitivity and specificity. *Nat. Mater.* **2011**, *10*, 602-607.
7. Yamamura, K.; Miyake, H.; Murata, I. Synthesis and properties of the cyclohexa[cd]perylenium tetrafluoroborate. A homolog of the phenalenium ion. *J. Org. Chem.* **1986**, *51,* 251-253.
8. Zou, W.; Visser, C.; Maduro, J.; Pshenichnikov, M. S.; Hummelen, J. C. Broadband dye-sensitized upconversion of near-IR light. *Nat. Photon.* **2012**, *6*, 560-564.
9. Pollnau, M.; Gamelin, D. R.; Lüthi, S. R.; Güdel, H. U. Power dependence of upconversion luminescence in lanthanide and transtion-metal-ion systems. *Phys. Rev. B* **2000**, *61*, 3337-3346.
10. Chen, G.; Somesfalean, G.; Liu, Y.; Zhang, Z.; Sun, Q.; Wang, F. Upconversion mechanism for two-color emission in rare-earth-ion-doped ZrO_2 nanocrystals. *Phys. Rev. B* **2007**, *75*, 195204.
11. Ye, S.; Li, Y.-J.; Yu, D.-C.; Dong, G.-P.; Zhang, Q.-Y. Room-temperature upconverted white light from $GdMgB_5O_{10}$:Yb^{3+},Mn^{2+}. *J. Mater. Chem. C* **2011**, *21*, 3735-3739.
12. van Swieten, T. P.; Yu, D.; Yu, T.; Vonk, S. J. W.; Suta, M.; Zhang, Q.; Meijerink, A.; Rabouw, F. T. A Ho^{3+}-Based Luminescent Thermometer for Sensitive Sensing over A Wide Temperature Range. *Adv. Opt. Mater*. **2021**, *9,* 2001518.